Iranian Journal of Science and Technology, Transactions of Mechanical Engineering (2022) 46:237–252
https://doi.org/10.1007/s40997-020-00418-w

RESEARCH PAPER

Reduction of Stress Variations on Sections (ROSVOS) for a Femoral Component

Levent Uğur[1] · Burak Ozturk[2] · Fehmi Erzincanli[3]

Received: 29 April 2020 / Accepted: 9 December 2020 / Published online: 18 January 2021

Abstract

Total knee prostheses have become established arthroplasty applications in the treatment of damaged or weakened cartilage. New implants are being produced using bio-materials which are compatible with human tissue. In the industry, these prostheses are modeled and manufactured in different design geometries. This study investigated using a novel method for an ideal geometry designed to prevent fracture problems caused by design errors and metallurgical weakness in femoral component geometry. This approach is presented in a flowchart demonstrating its implementation, orientation, and evaluation via finite element analysis. Unlike those in the literature, stress variations in the design surface cross sections were evaluated in this proposed design method, for different design types and angles. In this study, the design surface was divided into eight horizontal and ten vertical sections. The main objective of this study is to minimize the stress variations in these sections and to obtain the lowest possible volume value. As a result, stress exceeding the critical ratio was observed in four sections. In addition, three design parameters were found to be the most important for achieving maximum safety and minimum volume in this femoral component design. The method presented in this study aims to evaluate the ideal geometry of models and selection can be applied for the production of many industrial and biomechanical products.

Keywords Arthroplasty · Femoral component · Total knee prosthesis · Finite element method · ROSVOS

1 Introduction

Several prosthetic devices can be applied to compensate for cartilage tissue damaged as a result of various health problems. Prosthetic knee implants made of bio-materials are compatible with human tissue and have three main components: the tibial part, the femoral part, and the ultra-high molecular weight polyethylene (UHMWPE) insert located in between. Fluctuations inpatient weight over time as well as a deficiency in the microstructure of the material and fatigue wear may be led to damage of prosthetic devices (Laskin 1978). Consequently, unicompartmental knee arthroplasty (UKA) has become the established treatment for unilateral osteoarthritis of the knee since the early 1970s. However, preliminary outcomes of the procedure were not consistent (Laskin 1978; Insall and Aglietti 1980). Since then, UKA implementation and rates of survival have improved owing to better designs and advanced surgical techniques.

The average lifespan expected of a prosthesis is 15 years. When osteoarthritis has not expanded to involve other joints and the implant has not become loose, the case is considered to indicate the successful survival of the implant (Borus and Thornhill 2008). Contrarily, a knee prosthesis may prematurely cease to function due to such conditions mentioned above (Luring et al. 2006; Wada et al. 1997; Cameron and Welsh 1990; Sandborn et al. 1987; Veen and Raay 2014; Panousis et al. 2004; Boran et al. 2005). This is a correlation between material fatigue and patient weight (Luring et al. 2006; Wada et al. 1997). In one case, a patient became 38% heavier post-arthroplasty. In the patient, the component broke after a long period of sitting with the knee flexed to 90° and a sudden change of the knee flexion and loading. The weakened component was overloaded during the dynamic and weight-bearing process of the patient standing

✉ Burak Ozturk
burak.ozturk@bilecik.edu.tr

[1] Department of Mechanical Engineering, Amasya University, Amasya, Turkey

[2] Department of Metallurgy and Materials Engineering, Bilecik S. E. University, Bilecik, Turkey

[3] Department of Mechanical Engineering, Duzce University, Duzce, Turkey

up. This weight gain resulted in fatigue wear on the patient's implant, causing it to fracture.

Moreover, sections of high stress concentration were caused by continuous load on the sharp bend and thin metal (4 mm) of the design. As a result, the patient had to undergo a surgery in order to repair the broken implant almost nine years following his first arthroplasty (Fig. 1a) (Luring et al. 2006). Further research revealed three cases of femoral component stress fractures 32, 52, and 73 months post-UKA (Wada et al. 1997). The area was at the junction between the medial posterior beveled surface and the posterior flange. It is observed that the reason for the failure is due to the thinning of the metal at this point.

The bone leading to the cantilever bend was not supported and this may have led to the fracture of the anterior flange of the femoral part of the prosthesis in Fig. 1b. The prosthesis was surgically removed 11 years post-UKA. These issues might have been solved by adding a metal part to support that section of the femoral component (Cameron and Welsh 1990). Fractures at the maximum stress areas of two different sections of different products are shown in Fig. 1. It is thought that fracture on the prosthesis occurs due to the thinness of the geometry which results the inadequate material strength as well as high stresses in two different regions. Design problems arise in the stressed surfaces of many model geometries, especially the models without cement. There is a decrease in the strength properties of the implant due to microstructural defects. Also, safety coefficient decreases due to surgical errors as well as fractures in implant wear (Sandborn et al. 1987). Design deficiencies and improper placement of the prosthesis cause the prosthesis to loosen over time and increase stress. Therefore, it causes the components to fracture or wear (Veen and Raay 2014). Moreover, it has been reported that failures in design caused by the weakness of the material, inadequate specifications

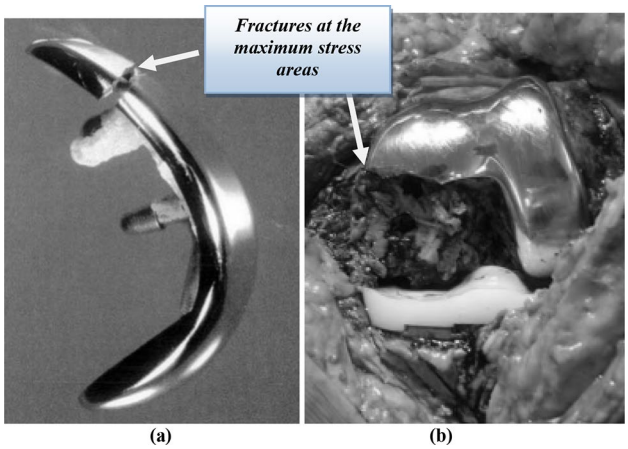

Fig. 1 Fractured femoral components (Luring et al. 2006; Cameron and Welsh 1990)

of the tibial component, and polyethylene insert (Panousis et al. 2004; Boran et al. 2005). Even though the accepted life expectancy of these implants is 15 years, a variety of fractures have been reported in total knee prosthesis (TKPs) (Luring et al. 2006; Wada et al. 1997; Cameron and Welsh 1990; Sandborn et al. 1987; Veen and Raay 2014; Panousis et al. 2004; Boran et al. 2005). In general, a review of the literature indicates that these fractures are a result of design geometry errors and patient weight gain post-surgery (Luring et al. 2006). Thin walls in the curved areas and areas subjected to stress are the main problem with the basic design geometry. Although research has been carried out on methods for measuring TKPs and for determining the optimum design geometry for minimum volume, it is observed that optimization of design geometry is not well covered (Veen and Raay 2014; Panousis et al. 2004; Boran et al. 2005). In addition to the clinical studies, earlier researches have developed options for the application of the classical finite analysis method (FEM). This study focused on developing a new design method inspired by previous studies. It is obtained affirmative results from optimization research on this proposed design (Küçük and Öztürk 2017; Küçük et al. 2017). Optimization studies in the design are applied in the development of design geometries in many different fields when the literature is researched. In particular, optimum design geometries are verified and developed by the finite element method (Öztürk and Erzincanli 2019; Heshmati and Amini 2020; Ghannadpour 2019; Pamnani et al. 2019).

A review of the literature was undertaken regarding research carried out using finite element analysis (FEA) and the development of design models for the optimization of prosthetic femoral components (Ilzarbe et al. 2008; Bahraminasab et al. 2014a, 2014b; Harrysson et al. 2007; Chandran et al. 2009; Huang et al. 2017; Willing and Kim 2009). Design of Experiments (DOE) and FEA techniques were used in the determination of factor levels conforming to a set of desirable specifications and in the creation of proposed steps for computational multi-criteria design experiments (Ilzarbe et al. 2008). Both FEA and response surface methodology (RSM) can be used to apply multi-objective design optimization of a functionally graded material (FGM) to a prosthetic femoral component (Bahraminasab et al. 2014a). The influence of material selection and geometric configuration was examined (Bahraminasab et al. 2014b). Their study investigated the performance of a total knee replacement (TKR) femoral component and the position of the pegs used in the design. In another study, a similar study was conducted. A unique custom-design method was proposed based on a scan of the patient's joint using computed tomography (CT). Their design featured a customized bone implant with articulating surfaces, thus seeking to avoid the problems linked to the traditional prosthetic knee components (Harrysson et al. 2007). Willing and Kim

used a parametric 3D FE model in their optimization of a UHMWPE insert design for TKR, with special emphasis on the problem of wear (Chandran et al. 2009). It is selected two designs for the anterior trochlear surface of their new femoral component: an anatomical V-shaped design (VSD) and a dome-shaped design (DSD) (Huang et al. 2017). While the V-shape design is mimicking the anatomical geometry of the anterior femur, the dome-shaped design is curve-on-curve articular surfaces for the patellofemoral joint. Many modeling studies in the literature involve optimization of TKP design geometry through alteration of width, size, and angle (Willing and Kim 2009; Dai et al. 2014; Dinçkal 2016; Desai 2019). It is used FEA to optimize a femoral cam-tibial post-articulation design and presented design parameters for optimization of femoral roll-back, with results showing pressure distribution of the tibial post (Willing and Kim 2009). The component fit was investigated for six groups of modern femoral component designs. They measured the overhang/underhang of the component in the resected distal femur and the size of the corresponding component and compared the findings for different designs and ethnic groups (Dai et al. 2014). The technique presented by researchers would enable preoperative determination of the most suitable type and size of implant to be used in a specific patient undergoing TKR. This demonstrates the potential of assisting surgeons to choose the optimum size and type of implant from among the range of those currently available (Dinçkal 2016; Desai 2019; Sun et al. 2016; Koziel and Bekasiewicz 2019). In addition to optimization studies on different designs and statistical methods of optimization (Cho et al. 2013; Öztürk et al. 2018; Williams et al. 2010), further studies on a variety of model designs can be found in the literature (Desai 2019; Sun et al. 2016; Koziel and Bekasiewicz 2019).

Researchers have proposed a parametric design method in the literature related to early fracture problems (Luring et al. 2006; Öztürk and Erzincanli 2019). This method statically interprets the effect of the change in each design parameter on the safety coefficient, allowing the development of optimum design geometry (Öztürk and Erzincanli 2019). In this method, different types of design geometries and angle changes during the operation of a prosthesis are not taken into account. It was determined only for the angle at which the maximum stress occurred and was evaluated statistically. The ROSVOS method allows to compare different types of design geometries and evaluating geometry for all working angles. Using the ROSVOS, the TKP will be able to demonstrate the maximum safety coefficient value for the ideal volume amount. For this purpose, variations in stress distribution on the surface exposed to engineering stresses were obtained by dividing horizontal and vertical sections at equal intervals. Thus, the optimum design could be obtained by reducing the difference between the maximum and the minimum amount of stress of each section.

2 Materials and Methods

The researchers believe that an optimum design can only be achieved by minimizing the variations in the amount of stress on the surface cross sections of the design. However, an optimum design can be modeled by considering all different design geometries and loading angles of a product. In the first step of this method, the ideal design geometry selection is made by comparing different types of design geometries with each other. Besides, the most critical horizontal and vertical surface sections where maximum stress occurs are determined. In the next step, this determined ideal design geometry is modeled with different parametric design options and analyzed via FEA. In the last step, the optimum design geometry is decided. Figure 2 shows the work flowchart with all parts and intermediate steps of the reduction of stress variations on sections (ROSVOS) method.

2.1 PART 1: Selection of Ideal Design Geometry

2.1.1 Determination of Different Model Types

In the first step of this proposed design development method, it is necessary to conduct a safety coefficient comparison among all model geometries. Figure 3 shows three commonly used design model geometries. According to geometry types, the M_1 design can be classified as progressive, the M_2 design as linear, and the M_3 design as radial. These three different types of design geometry were modeled in the Catia V5 program via the reverse engineering method. The volumes of these three types of design were 41,302, 38,821, and 39,715 mm^3, respectively.

2.1.2 Creation of Surface Sections of Model Geometries

Unlike the various design development methods, each design geometry is divided into a total of eight main sections and a technical drawing of each section is created (Fig. 4) in the ROSVOS method. Thus, the cross-sectional areas affecting the strength characteristics of each design geometry can be compared at this stage. When the cross-sectional pictures were examined, it was observed that a total of 24 different cross sections had areas that differed from each other. This method is based on the hypothesis that the optimum volume value can be obtained by reducing the stress changes in the sections. It is a method aimed at minimizing the difference between the minimum and maximum tensile amounts on specified cross-sectional lines at all operating angles of industrial products subjected to dynamic stress. Thus, the subtracted mass from the areas with high safety value is transferred to more unsafe areas. Thus, with the help of parametric design,

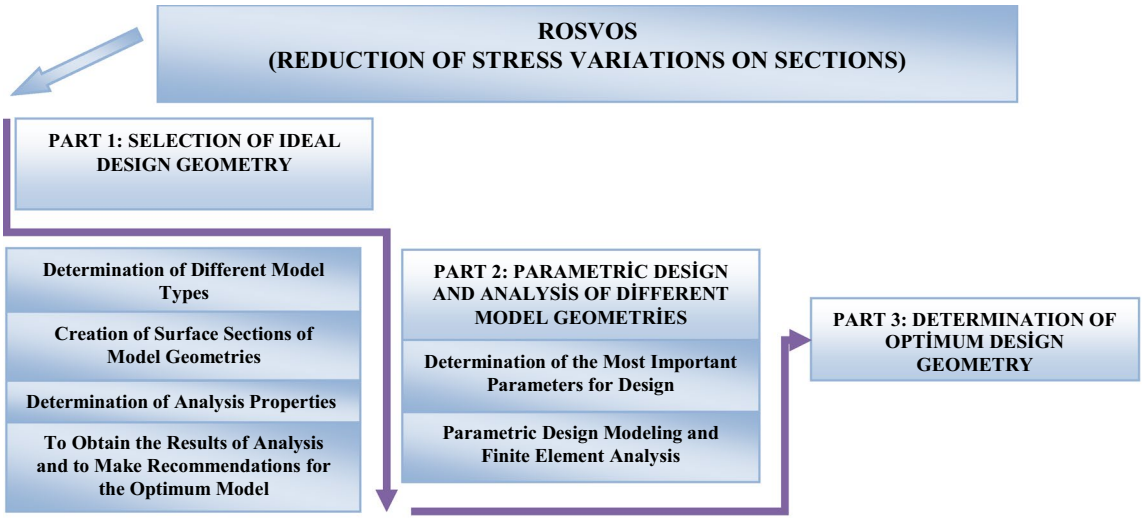

Fig. 2 ROSVOS method work flowchart

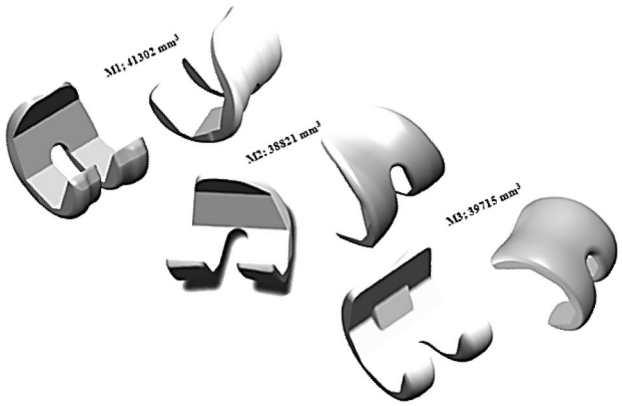

Fig. 3 Different types of TKP designs

designs with optimum volume and safety coefficient are obtained. To this purpose, the optimum design can be obtained by reshaping the volume and area of each section using parametric design. Therefore, stress amounts (MPa) were measured on a total of 80 different surface areas (8 × 10 sections) on the TKP surface (Fig. 5). While selecting these horizontal and vertical cross section lines, main geometry lines or surface transition regions in the design were chosen especially for shaping the design. Thus, the effects of changes in the design geometry in these regions on the amount of stress can be controlled and the ideal design geometry can be obtained.

2.1.3 Determination of Analysis Properties

The basic parts of the prosthesis are generally composed of titanium or cobalt–chrome metal alloy. The part that reduces the wear of two metal surfaces is made of polyethylene [ultra-high molecular weight polyethylene (UHMWPE)]. In this step of the proposed new model, all the properties required for a stress analysis by the FEM must be determined. References in the literature and the ANSYS program material library were applied to determine the mechanical properties of the Cr–Co–Mo and UHMWPE used in the FEM static analysis of engineering stresses (Table 1) (Villa et al. 2004). Compression stresses at different angles were obtained as a result of the dynamic loading of a knee prosthesis reported in the literature (Fig. 6) (Lundberg et al. 2012).

As indicated in Fig. 6, the TKP polyethylene insert performs a movement at an angle range of 0°–100°. Taking this kinematic motion into account, an analysis of the maximum amount of stress at angles of 20°, 40°, 60°, 80°, and 100° was required (Fig. 7). In the stress analysis for each angle, respectively, 2100, 1700, 1900, 2300, and 700 N forces were applied from the inner surface of the prosthesis. Stress distribution analyses of the three different models selected as TKP geometry were performed in the ANSYS 19.2 program. Each area was divided into 10 sections vertically and eight sections horizontally. The maximum amount of stress was calculated for a total of 80 different surface areas for each design geometry.

For mesh generation, the Solid187 tetrahedron element was used in the whole finite element model. A convergence analysis with mesh sizes from 5 down to 2 mm was accomplished. In our study, the maximum equivalent stresses on the plate and the maximum error energy were considered as convergence criteria. ϑ was the volume of the element, $\{\Delta\sigma\}$ was the nodal stress error, e was the error energy in element i, and $\{D\}$ was the stress–strain matrix. The nodal stress error $\{\Delta\sigma\}$ was the averaged nodal stresses minus the

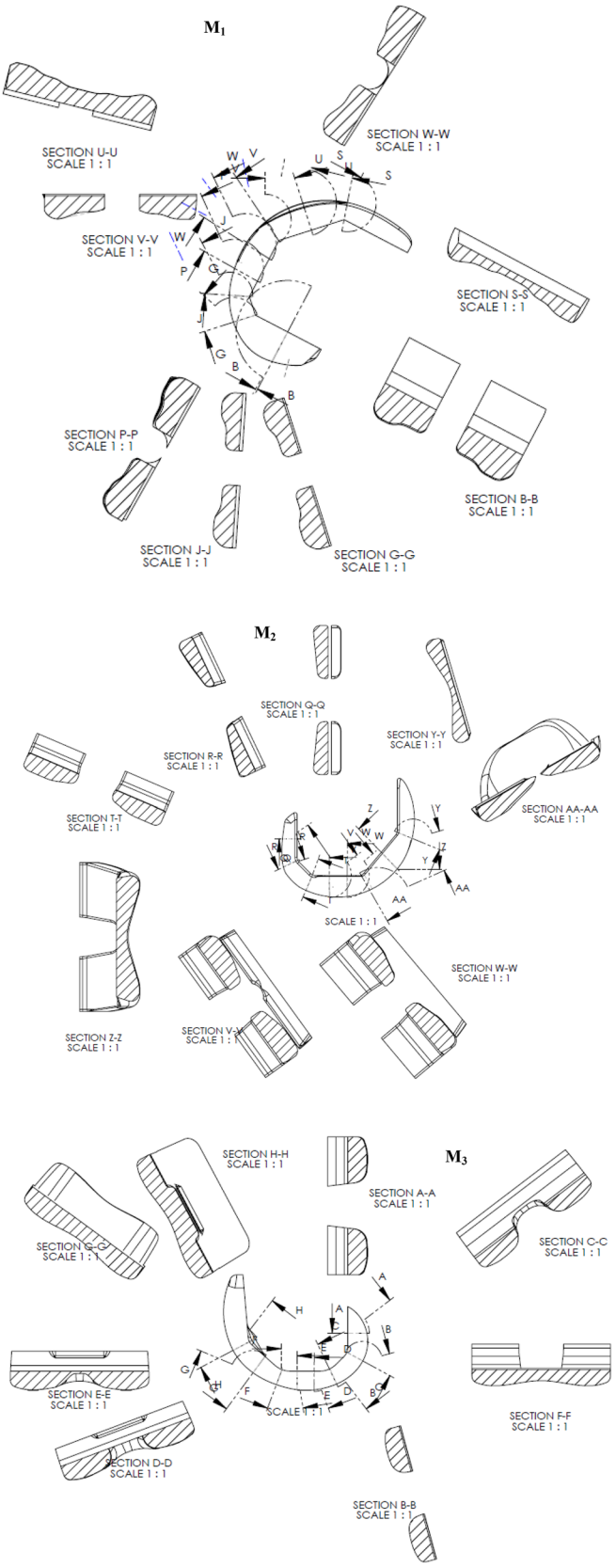

Fig. 4 Cross-sectional views of design types

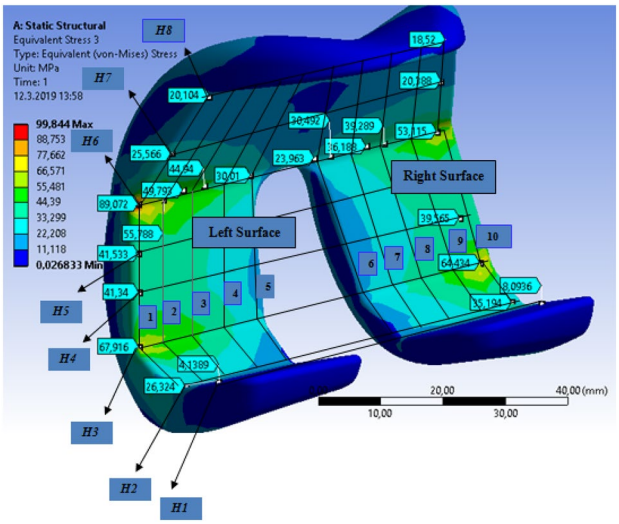

Fig. 5 Horizontal and vertical cross sections

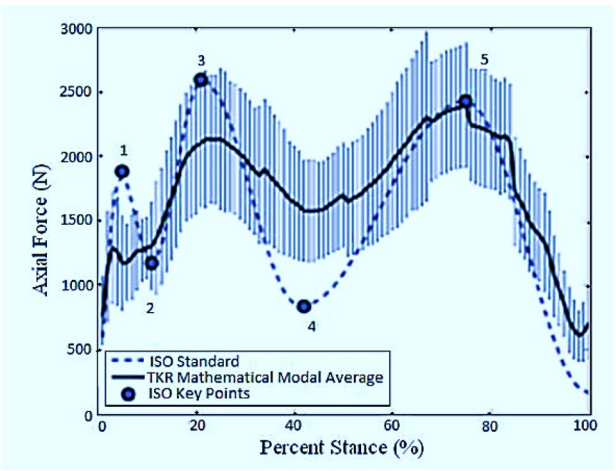

Fig. 6 Chart of axial forces on prosthesis as per ISO standards and TKR mathematical model average (Lundberg et al. 2012)

unaveraged nodal stresses (Ansys-Mechanical 2011; Steinbrück et al. 2014; Calisal and Ugur 2018).

$$e_i = \frac{1}{2} \int_{\vartheta} \{\Delta\sigma\}^T [D]^{-1} \{\Delta\sigma\} \mathrm{d}\vartheta. \quad (1)$$

2.1.4 Results of Analysis and Recommendations for the Optimum Model

In this part of the ROSVOS method, FEA is performed with all parameters defined in the analysis properties. The maximum stress results should be evaluated first. Thus, it can be determined at which angle and cross section intersection point on the model the maximum stress amount occurs (Figs. 8, 9, 10; Table 2).

2.2 PART 2: Parametric Design and Analysis of different Model Geometries

2.2.1 Determination of the Most Important Design Parameters

The average stress distribution in the horizontal surface sections is shown in Fig. 11 for the three different design models. The results revealed that the stress distribution

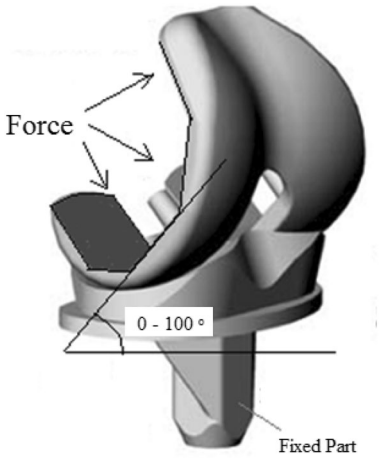

Fig. 7 Assembly design showing angles of stress analysis

was concentrated in two distinct parts. It was determined by a boundary line that the occurrence of stress was higher in sections 3, 4, 5, and 6 than in other sections. It was thought that by increasing the strength of the boundary line of the design geometry of the four sections, the amount of stress could be greatly reduced. These sections needed to be strengthened in terms of resistance, while the other sections did not need to be strengthened because this would only add unnecessary weight to the material.

Table 1 Mechanical properties of polyethylene insert (UHMWPE) and femoral component (Cr–Co–Mo) used in the analysis

Material	Density (kg/m^3)	Young's modulus (Pa)	Poisson's ratio	Yield strength (Pa)	Ultimate strength (Pa)
UHMWPE	930	6.90E+08	0.29	2.10E+07	4.80E+07
Cr–Co–Mo	8300	2.30E+11	0.3	6.12E+08	9.70E+08

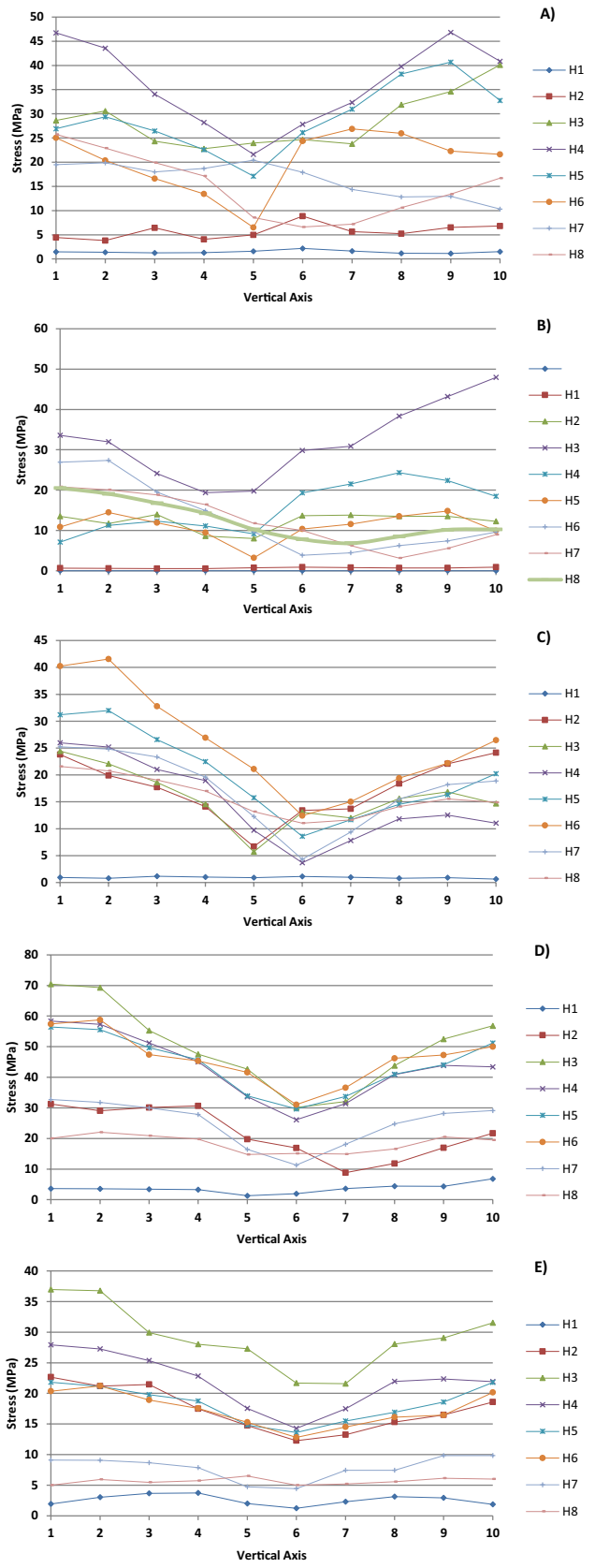

Fig. 8 Variations in stress on M_1 cross section. **a** 20°, **b** 40°, **c** 60°, **d** 80° and **e** 100°

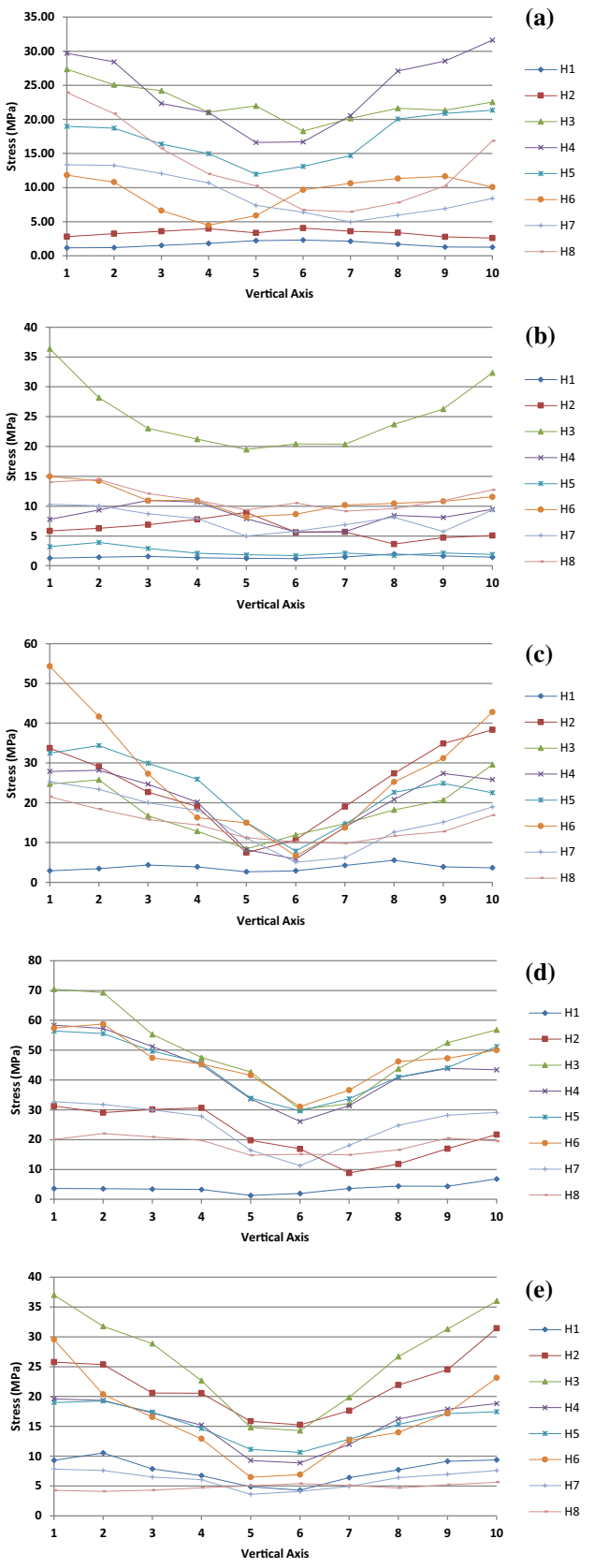

Fig. 9 Variations in stress on M_2 cross section. **a** 20°, **b** 40°, **c** 60°, **d** 80° and **e** 100°

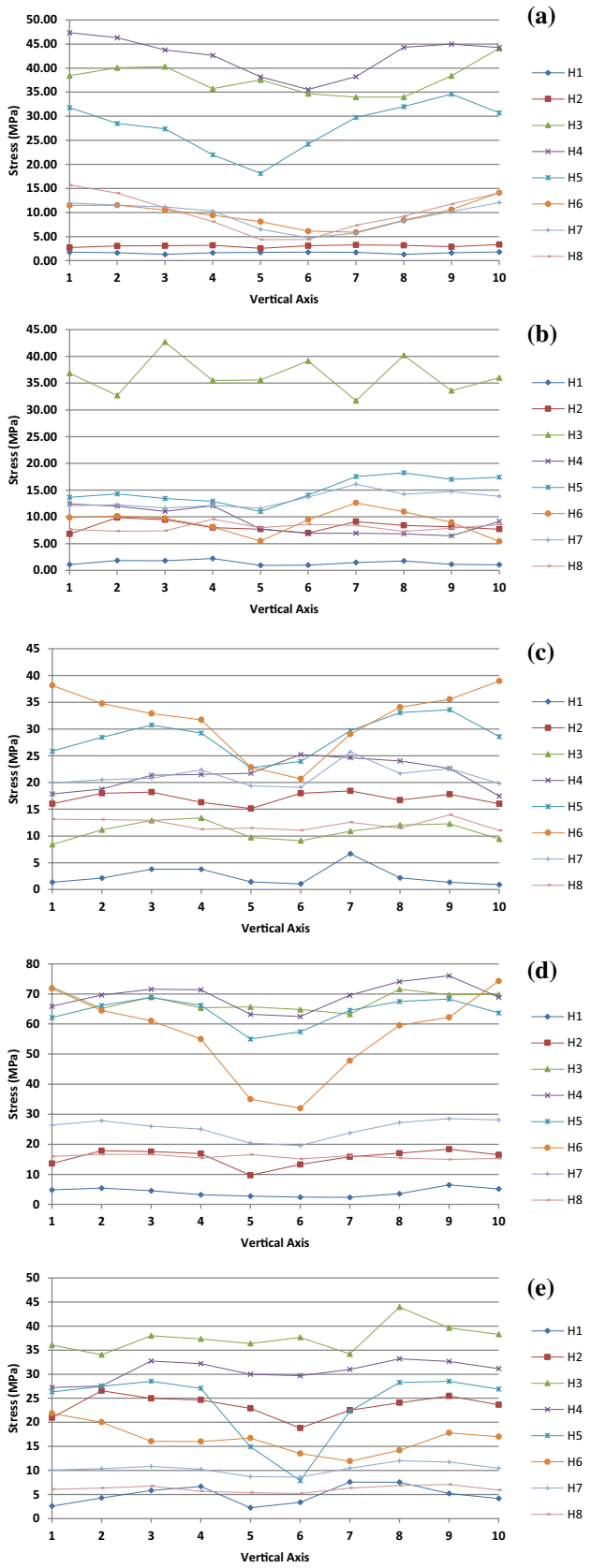

Fig. 10 Variations in stress on M_3 cross section. **a** 20°, **b** 40°, **c** 60°, **d** 80° and **e** 100°

Therefore, the other areas were not taken into consideration. All three different types of design geometry needed to be evaluated among each other to determine the ideal design type. The ideal design geometry was determined to be the second design type (M_2), in particular, because the amounts of volume and stress were the lowest (Fig. 11). It is observed that trends of graphs show abrupt changes for H_6, H_2 in the first figure, H_5, H_7 in the second figure, H_2, H_3 in the third figure. The major reason for these trends is the surface transitions on the design geometries. The external surfaces of the prosthesis should be modeled to perform basic knee movement. These design geometries are the most likely cause of changes in the amount of stress in the cross sections. It was observed that four different surface lines were of great importance for increasing the strength of the design. The sections from the 3rd to the 6th are the most important surface lines. Thus, the design geometry would need to be strengthened in the cross section where these four different maximum stresses occur. Increasing the safety coefficient in the four different sections of the M_2 design could only be achieved with the loft-cut feature depending on the specific parameters of this design (Fig. 12). This design geometry was modeled as a result of parametric modification of loft-cut draft drawings in five different planes. Thus, the safety coefficient and the variations in the volume of the design can be examined in detail in these four important cross sections shaped with different parametric designs shown in Fig. 13.

Loft-cut elements are widely used in almost all computer-aided design (CAD) programs. Generally, this command is used to extract or join multiple sections. This tool used in the creation of this prosthesis design allows us to obtain the final design based on a total of 16 variable parameters in five different sections. These design parameters are extracted from the main prosthesis body in the loft-cut process by way of multiple sections. The position of the radii and tangentially connected radii lines on the plane are identified and the measurement is completed. The experimental design prepared for different levels of 16 different design parameters is given in Table 3. These experimental design levels were selected in a mixed order and particular care was taken to ensure that the design parameters were not compromised when determining the lowest and highest levels for each of these design parameters.

2.2.2 Parametric Design Modeling and Finite Element Analysis

At this stage, the eight different design types determined in the experimental design were modeled and then the engineering stress analysis was performed via FEM. When comparing design types M_1, M_2, and M_3 with each other, it was observed that the highest amount of stress occurred at an

Table 2 Variations in stress values for 8 × 5 different areas (MPa)

		M_1V_1	M_1V_2	M_1V_3	M_1V_4	M_1V_5	M_2V_1	M_2V_2	M_2V_3	M_2V_4	M_2V_5	M_3V_1	M_3V_2	M_3V_3	M_3V_4	M_3V_5
H1	Left section	3.62	3.55	3.65	3.74	1.98	9.31	10.52	7.86	6.73	4.85	4.82	5.41	5.81	6.67	3.38
	Right section	6.93	4.37	4.43	3.66	2.19	9.38	9.12	7.69	6.39	4.29	5.15	6.51	7.52	7.57	2.78
	Average value	5.28	3.96	4.04	3.70	2.09	9.35	9.82	7.78	6.56	4.57	4.99	5.96	6.67	7.12	3.08
H2	Left section	31.26	29.09	30.15	19.77	16.91	33.72	29.04	30.15	30.69	19.77	20.94	26.54	24.07	22.5	22.89
	Right section	24.14	22.08	18.38	13.38	13.66	38.3	9.12	27.35	18.99	16.91	23.65	25.48	24.99	24.66	18.8
	Average value	27.70	25.59	24.27	16.58	15.29	36.01	19.08	28.75	24.84	18.34	22.30	26.01	24.53	23.58	20.85
H3	Left section	70.41	69.3	55.27	47.52	42.66	70.41	69.3	55.27	47.52	30.13	72.31	65.15	68.99	65.39	65.72
	Right section	56.85	52.5	43.84	32.08	29.81	56.85	52.5	43.84	32.08	42.66	69.84	69.7	71.58	63.29	64.85
	Average value	63.63	60.90	49.56	39.80	36.24	63.63	60.90	49.56	39.80	36.40	71.08	67.43	70.29	64.34	65.29
H4	Left section	58.34	57.29	51.22	45.1	33.69	58.34	57.29	51.22	45.1	33.69	65.92	69.66	71.61	71.39	63.25
	Right section	43.44	46.84	40.89	32.34	27.85	43.44	43.88	40.89	31.42	26.11	68.88	76.06	74.12	69.58	62.5
	Average value	50.89	52.07	46.06	38.72	30.77	50.89	50.59	46.06	38.26	29.90	67.40	72.86	72.87	70.49	62.88
H5	Left section	56.43	55.56	41.03	45.77	33.95	56.43	55.56	49.7	45.77	33.95	62.17	66.18	68.82	66.21	55.05
	Right section	51.19	44.1	49.7	33.74	29.67	51.19	44.1	41.03	33.74	29.67	63.73	68.28	67.53	64.54	57.4
	Average value	53.81	49.83	45.37	39.76	31.81	53.81	49.83	45.37	39.76	31.81	62.95	67.23	68.18	65.38	56.23
H6	Left section	57.43	58.73	47.41	45.34	41.62	57.43	58.73	47.41	45.34	41.62	71.82	64.47	61.07	47.83	35
	Right section	50.04	47.25	46.2	36.62	31.09	50.04	47.25	46.2	36.62	31.09	74.32	62.24	59.57	55	32
	Average value	53.74	52.99	46.81	40.98	36.36	53.74	52.99	46.81	40.98	36.36	73.07	63.36	60.32	51.42	33.50
H7	Left section	32.72	21.79	30.02	27.87	20.4	32.72	31.79	30.02	27.87	16.45	26.36	27.88	25.99	25.73	20.39
	Right section	29.11	28.19	24.81	18.11	17.91	29.11	28.19	24.81	18.11	11.34	28.15	28.54	27.2	25.06	19.58
	Average value	30.92	24.99	27.42	22.99	19.16	30.92	29.99	27.42	22.99	13.90	27.26	28.21	26.60	25.40	19.99
H8	Left section	21.59	22.06	20.93	19.78	14.81	23.94	22.06	16.58	19.78	14.81	15.69	16.68	16.62	16.2	16.6
	Right section	19.55	20.51	16.58	14.92	15.11	19.55	20.51	20.93	14.92	15.11	15.33	15	15.44	15.46	15.19
	Average value	20.57	21.29	18.76	17.35	14.96	21.75	21.29	18.76	17.35	14.96	15.51	15.84	16.03	15.83	15.90

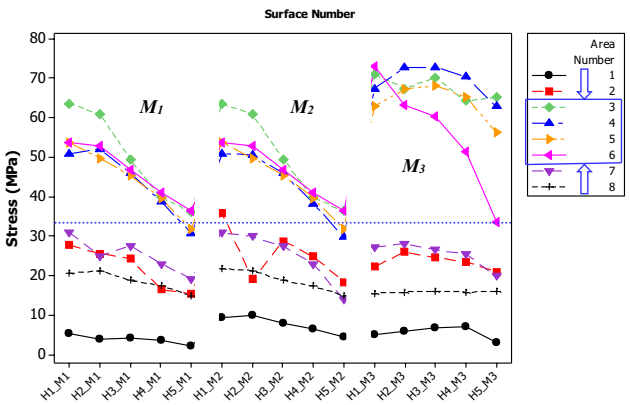

Fig. 11 Stress distribution graph for the three different designs

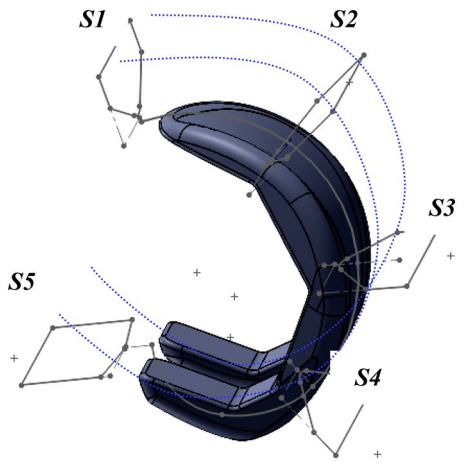

Fig. 12 Loft-cut sections forming the second type design (M_2)

angle of 80°. For this reason, these eight different types of design geometry were analyzed with the mounting designed at an 80° angle. Also, calculations were made in the ANSYS program under the same loads and with the defined material properties. The results of the stress variations in the four critical sections of these eight different design types are shown in Fig. 14. In the last step of this proposed design development method, the analysis results obtained at this stage were evaluated and the optimum design was obtained.

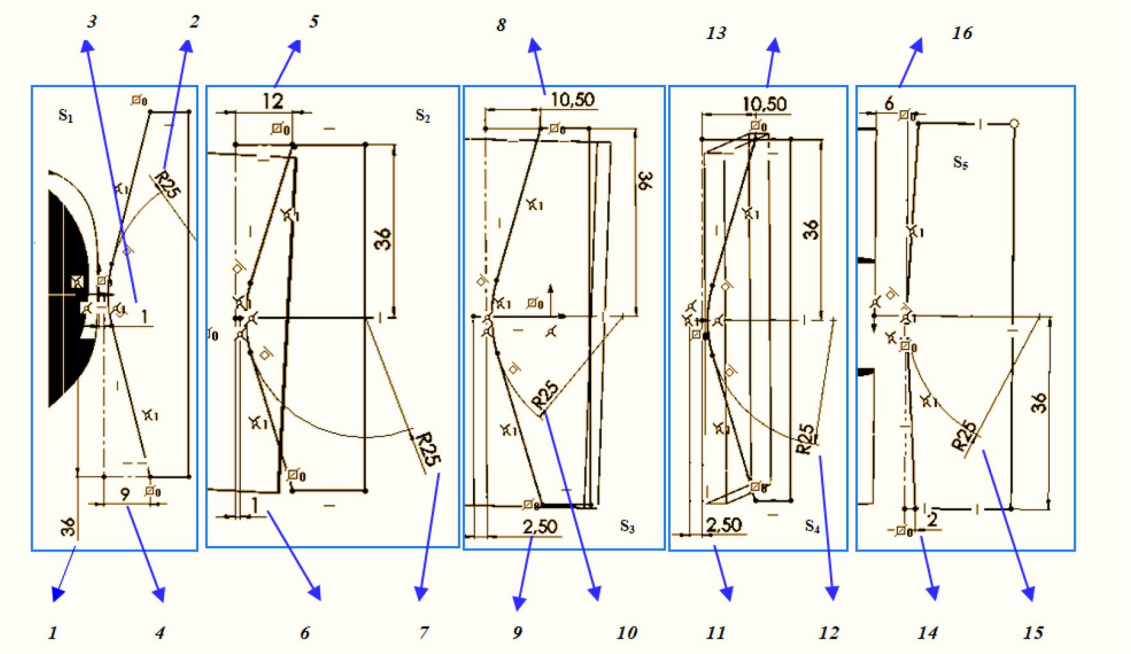

Fig. 13 Design parameters in five different sections

Table 3 Design parameters and levels

	P_1	P_2	P_3	P_4	P_5	P_6	P_7	P_8	P_9	P_{10}	P_{11}	P_{12}	P_{13}	P_{14}	P_{15}	P_{16}
M_1	36	25	1	9	12	1	25	10.5	2.5	25	2.5	25	10.5	2	25	6
M_2	36	25	1	9	13	1	35	11	2.5	35	2.5	35	10.5	2	25	6
M_3	36	25	2	9	12	2	25	10.5	3	25	3	25	10.5	2.5	25	6
M_4	34	35	2	9	12	2	35	10.5	3	35	3	35	10.5	2	35	6
M_5	34	35	1	10.5	14	1	35	11.5	2.5	35	2.5	35	11	2	35	5
M_6	34	35	0.5	11	14.5	0.5	35	12.5	1.5	35	1.5	35	12	2.5	35	5
M_7	34	35	0.5	11	14.5	1	45	12.5	1.5	35	1.5	45	12	2.5	35	5
M_8	34	35	0.5	11	13	0,5	45	12.5	1.5	35	1.5	45	11	2.5	35	5

2.3 PART 3: Determination of Optimum Design Geometry

At this stage of the ROSVOS method proposed by the researchers, the optimum design geometry is determined from among the geometries modeled in the experimental design. In order to better evaluate the stress variations in the cross sections of the eight different designs, the results are summarized in Table 4 and the average stress results are given. Of these design geometries, the design with the lowest volume was Design 1. The design with the lowest amount of stress was Design 3. However, the amount of stress of the first design and the volume value of the third design is very high. When the average stress variations of the four sections belonging to Design 6 were examined, it was determined that they varied between 36.27 and 26.20 MPa.

This variation in the geometry of the 1st design showed as 45.40–28.66 MPa. In the 3rd design, the average stresses in the cross sections were calculated in the range of 33.82–33.58 MPa. The 6th design model had a low average amount of stress and an average amount of volume. Moreover, the lowest value of variation between the amount of stress in the cross section was observed in this design geometry. At the same time, the other designs were examined. The results among the average cross-sectional stresses of the design types are very striking. However, the maximum amount of stress in the cross section of H_6 was very high, which is why this design was not chosen as the ideal design despite the volume and low average stress variations.

The effects of the levels of 16 different design parameters on the stress and volume variations in the four different critical stress zones are given in the matrix plot graph in Fig. 15. When these results were examined, it was found

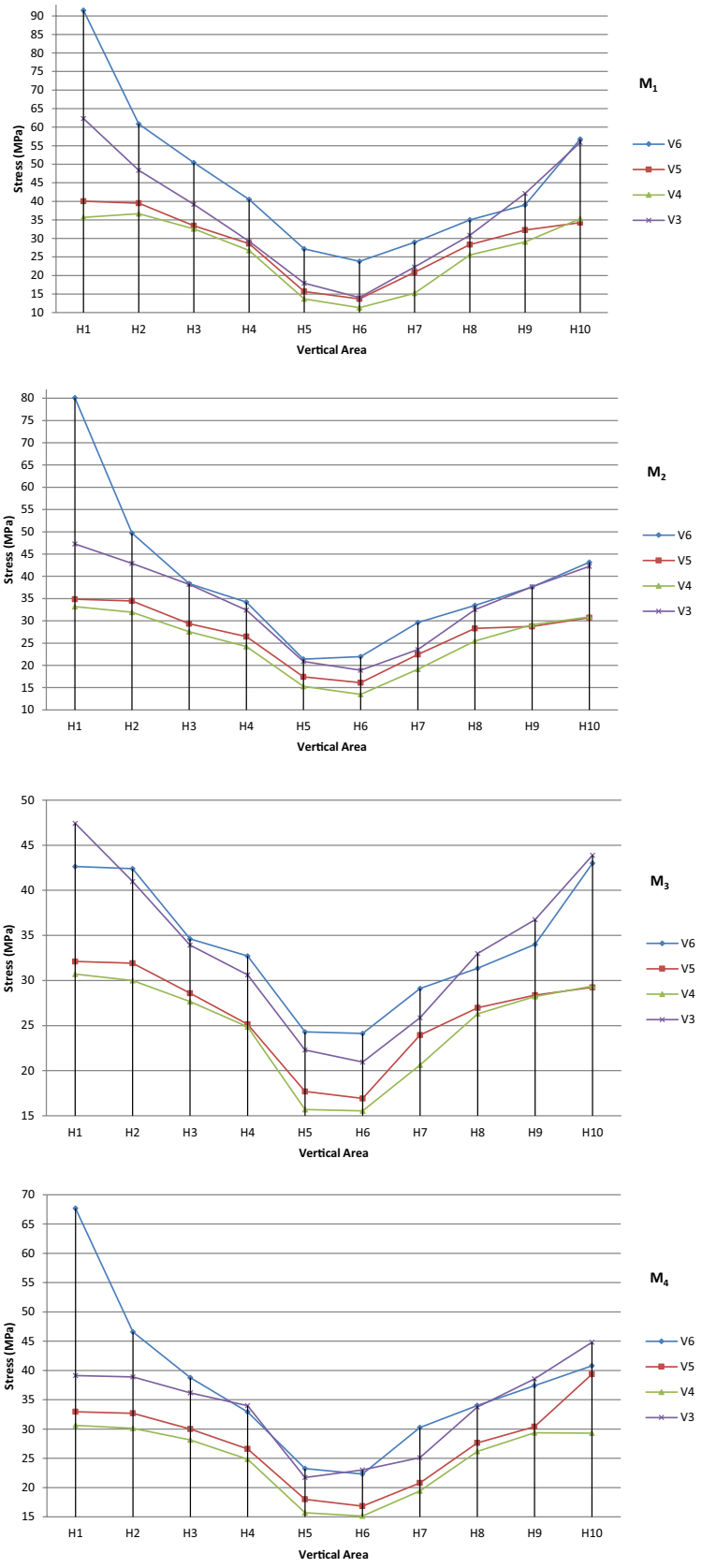

Fig. 14 Variations in stress on four different sections of eight different design types

Fig. 14 (continued)

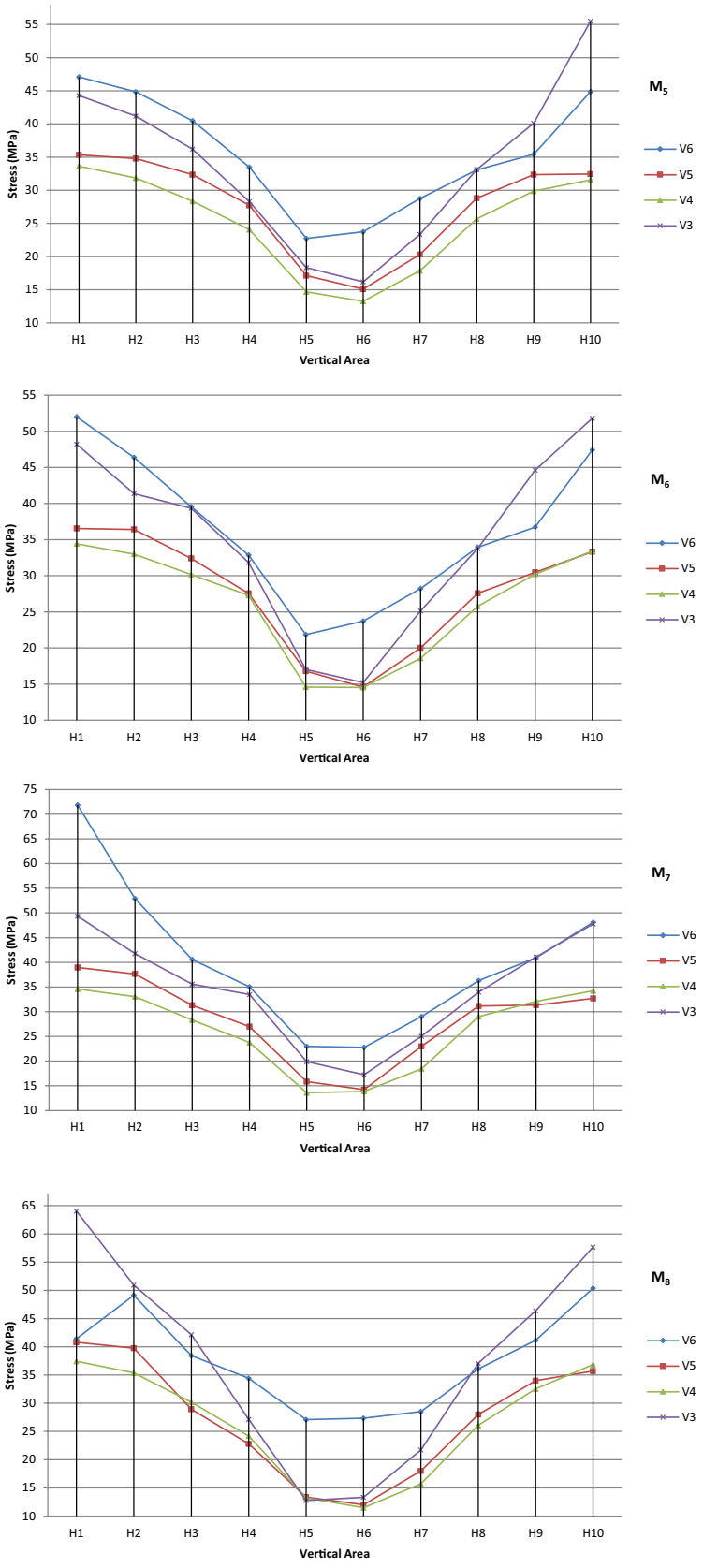

Table 4 Maximum stress results for all sections

		V1	V2	V3	V4	V5	V6	V7	V8	V9	V10	Average
M1 38824	H3	91.5	60.85	50.43	40.50	27.19	23.79	28.95	34.98	39.05	56.78	45.40
	H4	40.01	39.5	33.4	28.6	15.70	13.68	20.87	28.3	32.25	34.28	28.66
	H5	35.68	36.69	32.6	26.77	13.70	11.32	15.23	25.56	29.06	35.32	26.19
	H6	62.32	48.39	39.21	29.2	17.93	14.06	22.28	30.82	42.15	55.86	36.22
M2 41906	H3	80.1	49.74	38.34	34.22	21.41	21.97	29.61	33.47	37.62	43.17	38.97
	H4	34.85	34.47	29.34	26.46	17.41	16.12	22.44	28.29	28.72	30.69	26.88
	H5	33.18	31.93	27.58	24.23	15.26	13.49	19.14	25.46	29.13	30.86	25.03
	H6	47.26	42.89	38.19	32.40	20.88	18.89	23.56	32.51	37.64	42.23	33.65
M3 42351	H3	42.64	42.4	34.62	32.72	24.29	24.12	29.1	31.35	34	43	33.82
	H4	32.10	31.92	28.6	25.14	17.69	16.91	2.96	26.97	28.38	29.23	26.09
	H5	30.71	30	27.67	24.85	15.70	15.53	20.63	26.31	28.22	29.36	24.90
	H6	47.43	40.98	33.93	30.63	22.30	20.96	25.88	33	36.75	43.89	33.58
M4 43144	H3	67.67	46.58	38.77	32.91	23.26	22.31	30.25	34.01	37.40	40.78	37.39
	H4	32.96	32.67	30	26.61	18	16.83	20.78	27.62	30.38	39.35	27.52
	H5	30.64	30.14	28.13	24.85	15.70	15.14	19.41	26.16	29.36	29.28	24.88
	H6	39.14	38.89	36.16	33.97	21.71	23	25.12	33.74	38.56	44.81	33.51
M5 42440	H3	47.09	44.86	40.49	33.49	22.73	23.75	28.76	33.07	35.44	44.88	35.46
	H4	35.35	34.77	32.35	27.72	17.12	15.08	20.32	28.83	32.37	32.44	27.64
	H5	33.62	51.87	28.34	24.08	14.69	13.27	17.86	25.69	29.87	31.58	25.09
	H6	44.28	41.18	36.20	28.30	18.33	16.17	23.37	33.14	40.13	55.52	33.66
M6 41501	H3	52	46.39	39.54	32.86	21.86	23.73	28.21	33.95	36.73	47.42	36.27
	H4	36.55	36.40	32.39	27.55	16.77	14.58	20	27.58	30.48	33.32	27.56
	H5	34.42	33	30.17	27.27	14.58	14.54	18.58	25.77	30.2	33.43	26.20
	H6	48.19	41.37	39.34	31.83	17.03	15.2	25.13	33.77	44.63	51.82	34.83
M7 42487	H3	71.85	52.92	40.57	35.03	23	22.79	29.02	36.31	40.93	48.1	40.05
	H4	38.96	37.64	31.31	27	15.86	14.23	23	31.16	31.33	32.68	28.32
	H5	34.58	33.05	28.34	23.76	13.60	13.86	18.44	29	32.1	34.26	26.10
	H6	49.36	41.78	35.60	33.49	19.88	17.22	25.05	33.96	41.05	47.80	34.52
M8 40671	H3	41.43	49.14	38.44	34.42	27.08	27.34	28.53	36.09	41.13	50.38	37.40
	H4	40.79	39.75	28.95	22.80	13.35	12.02	18	28	34	35.71	27.34
	H5	37.45	35.38	30.17	24.17	13.22	11.47	15.72	26.10	32.54	36.84	26.31
	H6	64.05	50.94	42.16	27.12	12.78	13.32	21.73	37.08	46.4	57.66	37.32

that the P_1, P_3, P_6, P_9, $P_{11,}$ and P_{16} parameters increased the amount of volume, while generally decreasing the amount of stress in the sections. The P_5, $P_{10,}$ and P_{14} parameters reduced the amount of volume, while proportionally reducing the amount of stress in the cross section parameters, thus increasing the safety coefficient and minimizing the volume value. Selecting these maximum values will increase the safety coefficient value. The optimum design can be obtained by evaluating the other design parameters among each other. Using this proposed ROSVOS method, the optimum design model was determined without the need for statistical methods or theories. In making the selection for all parameter levels, the design geometry of the femoral component having the highest safety coefficient and a value close to the lowest volume was taken.

3 Conclusions

The development of a prosthesis with an optimum design means that lower weight, higher strength implant will be used throughout the life of the patient. Some models have been presented dealing with the optimization of design and material selection and process modeling of FEA studies. All of the design development methods related to these finite elements have not taken into account changes in stresses occurring in the geometry cross sections. In this novel study, the cross sectional alteration were examined for the first time both horizontally and vertically. Patient status reports indicate that industrial design geometries have not been developed with regard to precise criteria. In this study, the researchers proposed a new method which is about the evaluation of models and selection of ideal geometry which is practical and does not require any theoretical, statistical,

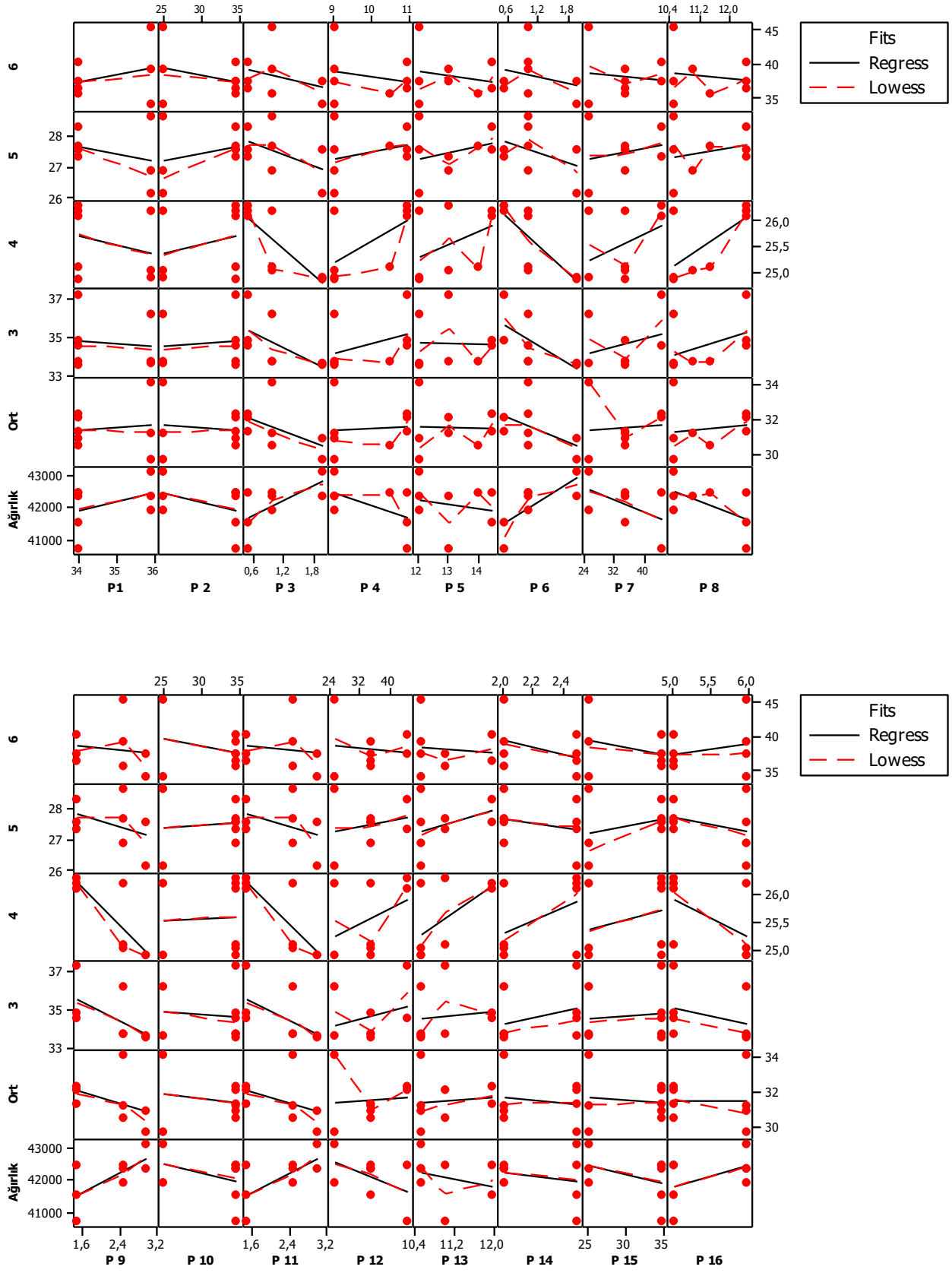

Fig. 15 Matrix plot showing the effects of design parameters on variations in stress and volume

or experimental research. In this study, ROSVOS metrology was applied to optimize the design of a femoral component and was described in detail with each intermediate step. The researchers calculated the amount of stress in Table 3 by applying the finite element method for 40 different nodes, located in the horizontal and vertical sections of prostheses with different volume values. When these results are examined, the effect of the force formed at each node and in different designs varied. As a result, the amount of safety coefficient of the product changes at the same rate. In M_4 geometry, which has the highest volume value among similar geometries, stress of 37.39 MPa occurred. However, although the volume value of M_6 geometry is 41501, the highest tension amount was measured as 36.27 MPa. These results show us that by distributing the volume value of a design per the sections, higher safety products with lower volume can be developed. Optimization of a femoral component design using this new method has yielded some conclusions, as listed below. Confirmation experiments were carried out to test the validity of the optimization, and the findings and conclusions were based on this context.

As a result of the ROSVOS method, the femoral component design geometry was improved by 6.8% and the safety coefficient of the product by 25.1%.

Eight different design types were developed using this method and consequently, the highest average stress in the overall design belonged to Design 1 (45.2 MPa). The average stress was the highest in Design 3 (33.82 MPa). In other words, the volume amount increased by 9%, and the safety coefficient was increased by 34.2%.

Four sections were determined to have high stress. The 3rd section was the part where the highest amount of stress occurred, whereas the section with the minimum amount of stress was the 5th section. These four sections were found to be fracture sites in the literature.

The parameters P_5, $P_{10,}$ and P_{14} were the most important parameters of the design for increasing the safety coefficient while decreasing the volume, i.e., increasing the safety with minimum volume. The internal radius value and the position on the plane were shaped using these parameters. Therefore, it is preferable that the external radius value is of a broad design.

Three different types of designs produced by the industry were compared in this research. When the stress variations in eight different horizontal cross sections of each model were examined, the cross sections of the 3rd, 4th, 5th, and 6th had a tensile value above 33 MPa, while the others had values well below that. It was determined that these sections were the parts that needed to be strengthened in terms of resistance, whereas the other sections needed to be reduced in volume. Moreover, the Design 2 model was the most ideal design type.

A prosthesis generally has a range of motion of 0°–100° and in this study, tensile analyses were performed for five different angles. The highest amount of stress was observed at an angle of 80° and the lowest amount of stress at an angle of 100°.

References

Ansys-Mechanical (2011) User-Guide: Ansys Reference Guide

Bahraminasab M, Sahari BB, Edwards KL, Farahmand F, Hong TS, Arumugam M, Jahan A (2014a) Multi-objective design optimization of functionally graded material for the femoral component of a total knee replacement. Mater Des 53:159–173

Bahraminasab M, Sahari BB, Edwards KL, Farahmand F, Jahan A, Hong TS, Arumugam M (2014b) On the influence of shape and material used for the femoral component pegs in knee prostheses for reducing the problem of aseptic loosening. Mater Des 55:416–428

Boran S, Hurson C, Synnott K, Keogh P (2005) Biomechanical analysis of tibial tray fractures post total knee arthroplasty. Eur J Orthop Surg Traumatol 15:295–299

Borus T, Thornhill T (2008) Unicompartmental knee arthroplasty. J Am Acad Orthop Surg 16:9–18

Calisal E, Ugur L (2018) Evaluation of the plate location used in clavicle fractures during shoulder abduction and flexion movements: a finite element analysis. Acta Bioeng Biomech 20(4):41–46

Cameron HU, Welsh RP (1990) Fracture of the femoral component in unicompartmental total knee arthroplasty. J Arthroplasty 5:315–317

Chandran N, Amirouche F, Gonzalez MH, Hilton KM, Barmada R, Goldstein W (2009) Optimisation of the posterior stabilised tibial post for greater femoral rollback after total knee arthroplasty—a finite element analysis. Int Orthop (SICOT) 33:687–693

Cho SH, Cho HL, Lee SH, Jin HK (2013) Posterior femoral translation in medial pivot total knee arthroplasty of posterior cruciate ligament retaining type. J Orthop 10(2):74–78. https://doi.org/10.1016/j.jor.2013.04.004

Dai Y, Scuderi GR, Penninger C, Bischoff JE, Rosenberg A (2014) Increased shape and size offerings of femoral components improve fit during total knee arthroplasty. Knee Surg Sports Traumatol Arthrosc 22:2931–2940

Desai A (2019) Ease of product assembly through a time-based design methodology. Assembly Autom 39(5):881–903. https://doi.org/10.1108/AA-09-2018-0133

Dinçkal Ç (2016) Free vibration analysis of carbon nanotubes by using finite element method. Iran J Sci Technol Trans Mech Eng 40:43–55. https://doi.org/10.1007/s40997-016-0010-z

Ghannadpour SAM (2019) A variational formulation to find finite element bending, buckling and vibration equations of nonlocal Timoshenko beams. Iran J Sci Technol Trans Mech Eng 43:493–502. https://doi.org/10.1007/s40997-018-0172-y

Harrysson OLA, Hosni YA, Nayfeh JF (2007) Custom-designed orthopedic implants evaluated using finite element analysis of patient-specific computed tomography data: femoral-component case study. BMC Musculoskel Disord 91:1–10

Heshmati M, Amini Y (2020) An electromechanical finite element model for new CNTs-reinforced harvesters subjected to harmonic and random base excitations. Iran J Sci Technol Trans Mech Eng 44:163–181. https://doi.org/10.1007/s40997-018-0254-x

Huang C-H, Hsu L-I, Chang T-K, Chuang T-Y, Shih S-L, Lu Y-C, Chen C-S, Huang C-H (2017) Stress distribution of the patellofemoral joint in the anatomic V-shape and curved dome-shape femoral component: a comparison of resurfaced and unresurfaced patellae. Knee Surg Sports Traumatol Arthrosc 25:263–271

Ilzarbe L, Alvarez MJ, Viles E, Tanco M (2008) Practical applications of design of experiments in the field of engineering: a bibliographical review. Qual Relia Eng Int 24(4):417–428

Insall J, Aglietti PA (1980) Five to seven-year follow-up of unicondylar arthroplasty. J Bone Joint Surg Am 62:1329–1337

Koziel S, Bekasiewicz A (2019) Fast multi-objective design optimization of microwave and antenna structures using data-driven surrogates and domain segmentation. Eng Comput 37(2):753–788. https://doi.org/10.1108/EC-01-2019-0004

Küçük Ö, Öztürk B (2017) Development of design geometry of aluminum fittings for healthy and safety sanitary installations. J Environ Prot Ecol 18:776–787

Küçük Ö, Öztürk B, Varhan S (2017) Investigation of the design parameters affecting the safety factor in fittings by using Taguchi method. The Turkish Journal of Occupational/Environmental Medicine and Safety: The 2nd international Water and Health Congress-Issue: The 2nd international Water and Health Congress, ISSN: 2149-4711, p 10

Laskin RS (1978) Unicompartmental tibiofemoral resurfacing arthroplasty. J Bone Joint Surg 60:182–185

Lundberg HJ, Ngai V, Wimmer MA (2012) Comparison of ISO standard and TKR patient axial force profiles during the stance phase of gait. Proc Inst Mech Eng H 226(3):227–234

Luring C, Perlick L, Schubert T, Tingart M (2006) A rare cause for knee pain: fracture of the femoral component after TKR. A case report. Knee Surg Sports Traumatol Arthrosc 15:756–757

Öztürk B, Erzincanli F (2019) Development of femoral component design geometry by using DMROVAS (design method requiring optimum volume and safety). Eng Comput 37(2):682–704. https://doi.org/10.1108/EC-03-2019-0077

Öztürk B, Uğur L, Erzincanlı F, Küçük Ö (2018) Optimization of polyethylene inserts design geometry of total knee prosthesis. Int Sci Voc Stud J 2:31–39

Pamnani G, Bhattacharya S, Sanyal S (2019) Numerical simulation of tri-layer interface cracks in piezoelectric materials using extended finite element method. Iran J Sci Technol Trans Mech Eng. https://doi.org/10.1007/s40997-019-00307-x

Panousis K, Murnaghan C, Koettig P, Grigoris P (2004) Fracture of the femoral component of a Brigham unicompartmental knee: a case report. Knee Surg Sports Traumatol Arthrosc 12:307–310

Sandborn PM, Cook SD, Kester MA, Haddad RJ (1987) Fatigue failure of the femoral component of a unicompartmental knee. Clin Orthop 222:249–254

Steinbrück A, Woiczinski M, Weber P, Müller PE, Jansson V, Schröder C (2014) Posterior cruciate ligament balancing in total knee arthroplasty: a numerical study with a dynamic force controlled knee model. Biomed Eng 13(1):91

Sun J, Shu L, Song X, Liu G, Xu F, Miao E, Xu Z, Zhang Z, Zhao J (2016) Multi-objective optimization design of engine crankshaft bearing. Ind Lubric Tribol 68(1):86–91. https://doi.org/10.1108/ILT-03-2015-0040

Van der Veen HC, Van Raay JJ (2014) Fracture of an Oxford femoral component: a case report. Knee 21:325–327

Villa T, Migliavacca F, Gastaldi D, Colombo M, Pietrabissa R (2004) Contact stresses and fatigue life in a knee prosthesis: comparison between in vitro measurements and computational simulations. J Biomech 37(1):45–53

Wada M, Imura S, Bo A, Baba H, Miyazaki T (1997) Stress fracture of the femoral component in total knee replacement: a report of 3 cases. Int Orthop (SICOT) 21:54–55

Williams DH, Garbuz DS, Masri BA (2010) Total knee arthroplasty: techniques and results. BCMJ 52(9):447–454

Willing R, Kim IY (2009) Three dimensional shape optimization of total knee replacements for reduced wear. Struct Multidisc Optim 38:405–414